



Determination of the critical micellar concentration of perfluorinated surfactants by cyclic voltammetry at liquid/liquid interfaces

Benjamín Nahuel Viada^{a, c}, Ana Valeria Juárez^{a, c}, Erica Marcela Pachón Gómez^{b, c}, Mariana Adela Fernández^{b, c}, Lidia Mabel Yudi^{a, c, *}

^a Universidad Nacional de Córdoba, Facultad de Ciencias Químicas, Departamento de Fisicoquímica, Córdoba, Argentina

^b Universidad Nacional de Córdoba, Facultad de Ciencias Químicas, Departamento de Química Orgánica, Córdoba, Argentina

^c Consejo Nacional de Investigaciones Científicas y Técnicas, CONICET, Instituto de Investigaciones en Fisicoquímica de Córdoba, INFIQC, Córdoba, Argentina

ARTICLE INFO

Article history:

Received 8 August 2017

Received in revised form

2 November 2017

Accepted 9 November 2017

Available online 12 January 2018

Keywords:

Perfluorooctanoic acid

Perfluorononanoic acid

Perfluorodecanoic acid

Critic micellar concentration

ITIES

Liquid/liquid interfaces

ABSTRACT

Based on the hypothesis that cyclic voltammetry applied to the interface formed by two immiscible electrolyte solutions can be used for determining critical micellar concentrations (cmc) of charged surfactants provided they exhibit ion transfer currents, we have carried out the study of three perfluorinated acids (perfluorooctanoic acid, PFO, perfluorononanoic acid, PFN, and perfluorodecanoic acid, PFD), dissolved in the aqueous phase. Cyclic voltammetry at the water/1,2-dichloroethane interface as well as fluorescence and surface pressure measurements, have been employed for cmc determinations and comparison. From the variation of voltammetric parameters on surfactant concentration it was possible to determine the cmc for these surfactants, obtaining good agreements with other methodologies. Impedance spectroscopy experiments have been also carried out to characterize the properties of the interface, demonstrating that at high surfactant concentration values, a monolayer with different domains is formed.

© 2018 Elsevier Ltd. All rights reserved.

1. Introduction

Due to the wide range of applications related with surfactant adsorption at different interfaces, the critical micellar concentration (cmc) is the simplest and one of the more important parameters for the characterization of colloid and surface properties of surfactant species, which also determines its industrial usefulness, such as foaming, wetting, emulsification and solute solubilization [1].

Several experimental methods for the determination of cmc of surface-active agents have been developed, all of them based on the discontinuity or inflection point in a measurable physical property of the solution as the surfactant concentration is increased [2–5].

Electrochemical techniques at solid/liquid interfaces have been successfully used for studying different properties of these organized structures, such as diffusion coefficients, micellar hydrodynamic radius, cmc [6–8], aggregation number of reverse micelles,

amount of micelles forming droplet clusters and standard electron transfer heterogeneous rate constants [9]. Electrochemistry at liquid/liquid interfaces, formed between two immiscible electrolyte solutions, has also been employed for studying the interfacial behavior of different surfactants. Special interest has been paid to the study of the adsorption of phospholipids and ion transfer across these monolayers [10–16]; the effect of surfactants on fusion of emulsion particles to the interface [17]; as well as the transfer of cationic surfactants, employed as template species for the generation of mesoporous silica deposits [18–22], and the use of micelles for the amperometric detection of proteins at liquid/liquid interfaces [23].

Fluorinated surfactants have been extensively used in different industrial applications due to their unique properties such as their higher surface activity and stability compared to the corresponding hydrocarbon compounds. Motivated by these unique properties of perfluorinated surfactants, numerous investigations have focused on the study of their adsorption at different interfaces [24], and the micellar systems formed by these species [25,26] or by their mixtures with hydrocarbon surfactants [27].

The aim of the present paper is to study the transfer of perfluorinated acids through a polarized water/1,2-dichloroethane and

* Corresponding author. Universidad Nacional de Córdoba, Facultad de Ciencias Químicas, Departamento de Fisicoquímica. Consejo Nacional de Investigaciones Científicas y Técnicas, CONICET, Instituto de Investigaciones en Fisicoquímica de Córdoba, INFIQC, Córdoba, Argentina.

E-mail address: mjudi@fcq.unc.edu.ar (L.M. Yudi).

to demonstrate that the variation of voltammetric parameters with surfactant concentration in combination with impedance spectroscopy experiments provide useful information related to the interfacial and micellar properties.

2. Experimental

2.1. Materials and electrochemical cell

A four-electrodes system employing a conventional glass cell of 0.17 cm² interfacial area was used for the electrochemical measurements. The reference electrodes were Ag/AgCl and two platinum wires were used as counter electrodes. The reference electrode corresponding to the organic phase was immersed in an aqueous solution composed of 10.00 mM tetrapentylammonium bromide (TPnABr, Sigma-Aldrich) and 10.00 mM LiCl. All potential values (E) reported in this work are those which include $\Delta\phi_{tr, TPnA^+}^0$ for the transfer of TPnA⁺ as reference ion.

The base electrolytes solutions were 10.00 mM LiCl (p.a. grade) in ultra-pure water and 10.00 mM tetrapentylammonium tetrakis (4-chlorophenyl) borate (TPnATCIPB) in 1,2-dichloroethane (DCE, Dorwill p.a.). TPnATCIPB was prepared by metathesis of TPnABr and potassium tetrakis (4-chlorophenyl) borate (KTCIPB, Sigma - Aldrich p.a.).

The surfactants perfluorooctanoic acid (PFO), perfluorononaic acid (PFN) and perfluorodecanoic acid (PFD) were purchased from Sigma – Aldrich and employed without further purification (purity: 98%). These acids were added to the aqueous phase in a concentration range from 0.05 mM to 3.00 mM. All experiments were carried out at pH = 6.00, at this pH value, the three surfactants are completely ionized in water, in their anionic form with their polar head group negatively charged.

In this way, the electrochemical cell employed was as follows:

Ag	AgCl	TPnABr	TPnATCIPB	LiCl	AgCl	Ag
		10.00 mM (w')	10.00 mM (o)	10.00 mM (w)		
				PFO, PFN or PFD 0.05-3.00 mM		

2.2. Cyclic voltammetry (CV) and electrochemical impedance spectroscopy (EIS) experiments

A four-electrode potentiostat with periodic current interruption for automatic elimination of solution resistance was used for CV experiments. The potential was changed from 0.150 V to 0.900 V with a waveform generator (Hi-Teck Instruments). Voltammograms were recorded employing a 10 bit computer board acquisition card connected to a personal computer. The voltammograms were obtained with typical errors of $\pm 10\%$ in current values.

EIS experiments were carried out employing an electrochemical analyzer CHI C700. The data acquisition and processing were made with ZPlot/Zview (Scribner Associates Inc.) program. The frequency range was 0.1–2000 Hz, the amplitude of the ac perturbation was 10 mV and different constant dc potential, E , were applied.

Capacitance (C) vs E curves were also recorded at the frequency value corresponding to the maximum of Bode plots (phase angle vs frequency).

2.3. Surface pressure - molecular area isotherms and surface pressure – concentration curves

A mini-trough II from KSV Instruments Ltd. (Helsinki, Finland) was used to obtain the surface pressure - molecular area isotherms for the three surfactants analyzed. The surface tension was measured using the Wilhelmy plate method with a platinum plate.

The aqueous subphase was 10.00 mM LiCl placed in a Teflon trough (364 mm \times 75 mm effective film area). For the compression experiments (surface pressure vs molecular area isotherms), 100 μ L of 0.70 mM PFO, PFN or PFD solutions in 1:2 methanol:chloroform were spread at the air/water interface employing a Hamilton micro-syringe. Before spreading these solutions, the subphase surface was cleaned by sweeping it with the Delrin barriers and then any surface contaminant was removed by suction from the interface. The cleaning of the surface was checked by recording an isotherm in the absence of the surfactants and verifying a surface pressure value lower than 0.20 mN m⁻¹. After spreading, the solvent was allowed to evaporate by 10 min, and then the film was compressed with two barriers at a compression speed of 5 mm min⁻¹, while the automatic measurement of the lateral surface pressure (π) was carried out.

For analyzing the variation of surface pressure with surfactant concentration, successive volumes of 5 μ L of 0.100 M PFO, PFN or PFD aqueous solutions were injected to a 10.00 mM LiCl subphase, contained in a cell with a constant surface area equal to 3.94 cm², while the stationary surface pressure value was recorded for each concentration. In this way, surfactant concentration values within the range 1.00–4.00 mM were attained.

2.4. Fluorescence measurements

Fluorescence experiments were carried out employing 8-anilinoanthracene-1-sulfonate (ANS) as fluorescence probe at

constant concentration equal to 0.14 mM. The variation of fluorescence intensity (F) as a function of surfactants concentration was analyzed within the range 1.00 mM $< c_{\text{surfactant}} < 3.00$ mM.

ANS emission spectra and fluorescence emission intensities at $\lambda = 475$ nm were recorded employing a Perkin Elmer LS 55 fluorescence spectrophotometer by exciting at 370 nm.

2.5. Determination of aggregation numbers

The aggregation numbers of the perfluorinated surfactants were determined by quenching of the fluorescence of Pyrene. The measurements were performed with a Perkin Elmer LS 55 fluorescence spectrophotometer using a 1 cm optical path length quartz cuvette. The concentration of the probe (Pyrene, Fluka 98%) was maintained constant ($c_{\text{pyrene}} = 2.0 \mu\text{M}$) whereas the quencher concentration was varied from 50.0 to 600.0 μM (quencher: cetylpyridinium bromide, Aldrich 98%), maintaining a constant concentration of the perfluorinated surfactant above their cmc. Pyrene is hardly soluble

in water, for this reason the stock solution of this probe was prepared in methanol, so that, the final pyrene solutions contained methanol at 0.4 vol %. Before the determinations, the solutions were shaken for 24 h at 25 °C in a thermostated bath to attain solubilization equilibrium. Pyrene was excited at 335 nm and the bandwidths of the excitation and fluorescence slides were both set as 3.0 nm. The measurements were carried out at (25.0 ± 0.1) °C.

3. Results and discussion

3.1. Critical micellar concentration (cmc) determined by cyclic voltammetry

Fig. 1 shows the voltammograms obtained for the anionic form of the three fluorinated surfactants analyzed in the present paper, PFO^- , PFN^- , PFD^- . These anions are transferred from the aqueous to the organic phase, during the negative potential scan, at potential values $E_p(-) = 0.410$, 0.425 and 0.475 V respectively. The gradual shift of peak potentials towards negative values as the chain length decreases is due to decrease in the hydrophobicity. For the three anions, peak current values are proportional to square root of scan rate, while peak potentials and $\Delta E_p = E_p(+)-E_p(-)$, equal to 0.060 V, are constant within the whole scan rates range analyzed. These results allow concluding that the transfer of the three anions is reversible and diffusion controlled.

Fig. 2 shows the voltammograms obtained when PFN^- is present in aqueous phase at different concentrations. A single peak system is observed at low concentrations of surfactant (Fig. 2a). Under these conditions a linear relationship between peak current and anion concentration was obtained and, from the slope of this plot the diffusion coefficient of PFN^- in aqueous phase was determined. Similar behaviors were observed for PFO^- and PFD^- and the diffusion coefficient values calculated are listed in Table 1 for the three anions. As the concentration increases, a second peak system is evident at more negative potential values, as can be noted in Fig. 2 b) – d). Also in this case a linear relationship of peak current with square root of scan rate and with surfactant concentration (not shown) was observed. Three different processes could be responsible for this second peak: 1) the facilitated transfer of TPnA^+

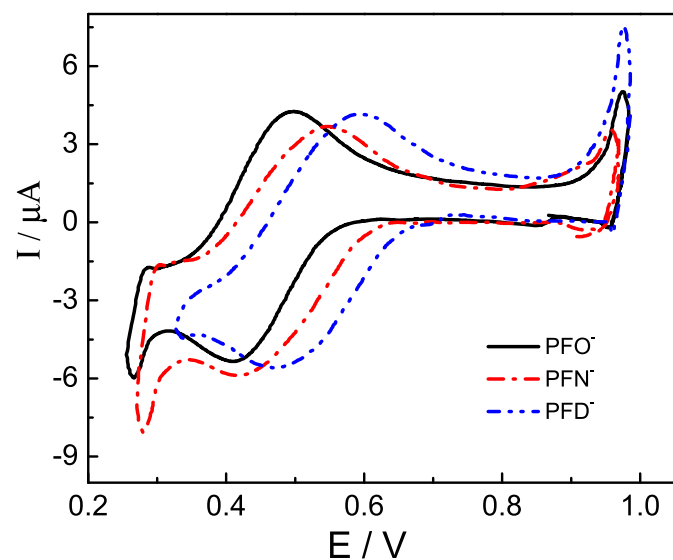


Fig. 1. Cyclic voltammograms for PFO^- (—), PFN^- (---) and PFD^- (- · -) transfer at the water/1,2-dichloroethane interface. Aqueous phase composition: 0.25 mM perfluorinated acid +10.00 mM LiCl. Organic phase composition: 10.00 mM TPnATCIPhB . $v = 0.050$ V s^{-1} .

present in the organic phase, by interfacial ionic pair formation with the negatively charged surfactants present in the aqueous phase, 2) the transfer of pre-micellar structures, whose formation is favored at high surfactant concentrations, occurring at more negative transfer potential compared to that corresponding to the monomeric form of the surfactant; this fact can be explained taking into account that the association of two or three surfactant molecules leads to a more hydrophilic species due to the higher negative charge on the aggregates, provided by the polar head groups, and also by the fact that hydrophobic chains remain hidden from the aqueous medium; 3) considering that the increasing surfactant concentration leads to the adsorption of these molecules at the interface, the second peak could be due to desorption of surfactant molecules from the interface to the organic phase. In order to determine which of both processes corresponds to the second peak, the surface pressure, in the presence of a surfactant concentration equal to 0.50 mM, was recorded, before and after applying a potential step at $E = 0.250$ V during 30 s. At this concentration value, the second process is evident and, in the case that desorption process would be occurring, important changes in surface pressure values should be observed after a potential step at $E = 0.250$ V. Fig. 3 shows the changes in surface pressure ($\Delta\pi = \pi - \pi_{\text{initial}}$, where π_{initial} correspond to the initial surface pressure before any perturbation while π is the pressure recorded during or after the perturbation) obtained before, during and after the step at $E = 0.250$ V. Fig. 3 shows the changes in surface pressure ($\Delta\pi = \pi - \pi_{\text{initial}}$, where π_{initial} correspond to the initial surface pressure before any perturbation while π is the pressure recorded during or after the perturbation) obtained before, during and after the step at $E = 0.250$ V (full line). It is worth noting that the initial potential, before the application of the step, was the equilibrium open circuit potential. The response observed in the absence of the surfactant (dashed line) is also included for comparison. The ascending arrows indicate the beginning of the potential step and the descending arrows the end of the step. As can be noted, there is no a significant decrease in the pressure during the potential step as might be expected if a desorption process was occurring under these polarization conditions. The decrease in pressure observed after the step, corresponding to barely 0.06 mN m^{-1} , both in the absence and in the presence of the surfactant, may be due to interface rearrangement. Besides, the linear dependence of current peak with $v^{1/2}$ observed for the second process (not shown) indicates a diffusion controlled transfer reaction. These both evidences could be confirming that the second peak corresponds to the transfer of pre-micellar species or to the ionic pair formation between TPnA^+ cations and perfluorinated anions and could allow to discard the possibility of desorption of surfactant molecules from the interface to the organic phase.

If PFN^- concentration continues to increase, and values equal to or greater than 2.24 mM are reached, a sudden change in the shape of the voltammogram occurs as can be observed in Fig. 4. The normalization of the current by the concentration values allows to better clarifying the effect of increasing the surfactant concentration. A sharp increase in the negative current along with a stationary shape response, at low scan rate, is evident for these high concentrations. This sudden change in voltammetric response is assigned to the micelle formation. On one hand the sharp increase in current is due to the increase in the negative charge of the transferred species and, on the other hand, the stationary current observed at low scan rates can be explained considering that an important amount of surfactants molecules are adsorbed at the interface. At this point, it is worthwhile to remark that ion transfer processes on modified interfaces, by surfactants adsorption, can take place in different ways [28]. On homogeneous films, ion transfer across the film is possible by permeation, and kinetic control will appear in the electrochemical process. If the distribution of adsorbing molecules is not uniform, with blocked and bare domains (pinholes), the ion transfer can occur both, by the above mechanism and through clean surface spots. In the last case, the

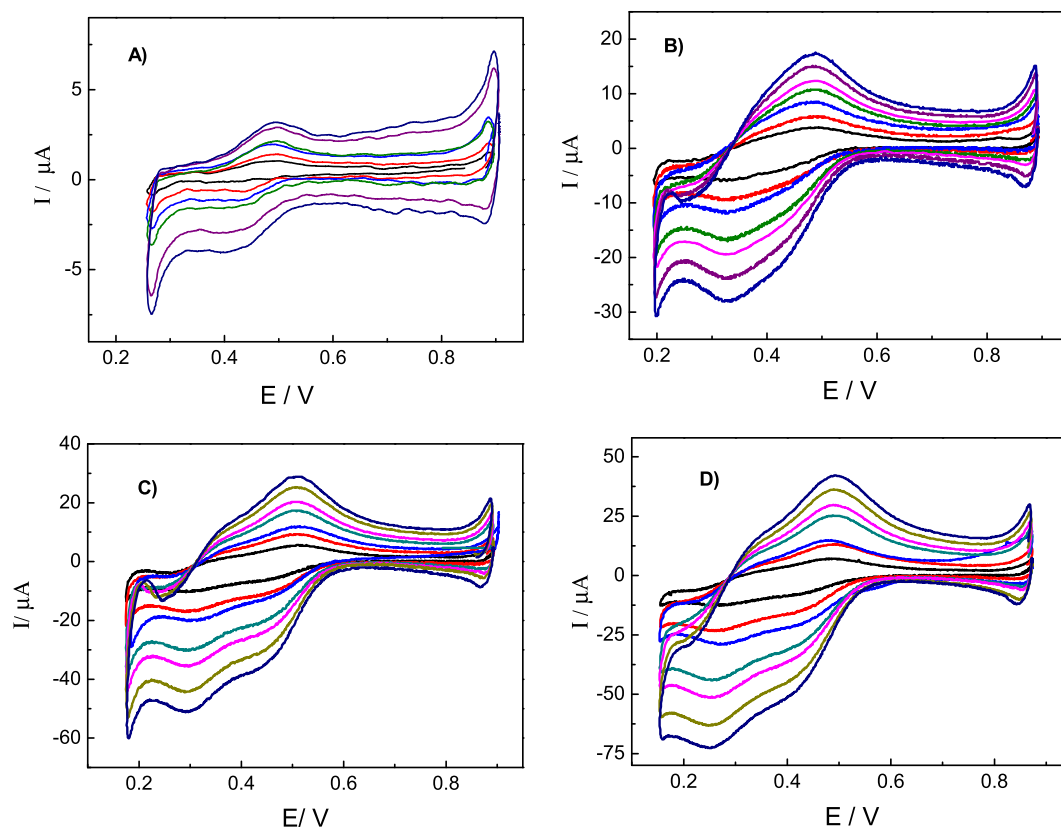


Fig. 2. Cyclic voltammograms for PFN^- transfer at the water/1,2-dichloroethane interface. Aqueous phase composition: 10.00 mM LiCl + PFN at different concentrations: A) 0.05 mM, B) 0.32 mM, C) 0.74 mM and D) 0.95 mM. Organic phase composition: 10.00 mM TPnATCIPhB. $v = 0.010, 0.025, 0.050, 0.075, 0.100, 0.150$ and 0.200 Vs^{-1} .

Table 1
Diffusion coefficient (D) for the surfactants studied (PFO^- , PFN^- and PFD^-) at monomeric and micellar forms.

	Diffusion coefficient ($D/\text{cm}^2\cdot\text{s}^{-1}$)	
	Monomeric surfactants	Micelles
PFO	$1.44\cdot 10^{-5}$	$2.4\cdot 10^{-6}$
PFN	$1.29\cdot 10^{-5}$	$4.46\cdot 10^{-6}$
PFD	$1.19\cdot 10^{-5}$	$7.76\cdot 10^{-6}$

voltammetric response depends on size, distribution and number of pinholes and on the time scale of the experiment, as stated by the theoretical models for diffusion behavior at microelectrode assemblies [29–31]: at high scan rates, when the microhole diameter, ϕ , is higher than the diffusion layer thickness, δ , a semi infinite linear diffusion should occur and the typical peaked shape voltammogram should be observed. As scan rate decreases and δ is large compared to ϕ , but small compared to the distance d between two adjacent microholes, spherical diffusion to individual pinholes occurs and a stationary shape voltammogram should be observed.

The steady - state wave response observed for PFN^- at low sweep rates during the negative sweep rate, evidences a spherical diffusion process. This result would be demonstrating the presence of uncovered microholes at the interface, where the PFN^- transfer process takes place. The peaked shape of the process observed during the reverse scan and the lower peak current values compared to those of forward process could be explained considering that micelles are disaggregated in the organic phase and the monomeric species, or other structures of surfactant are transferred to the aqueous phase at the corresponding $E_p(+)$. If scan rate is

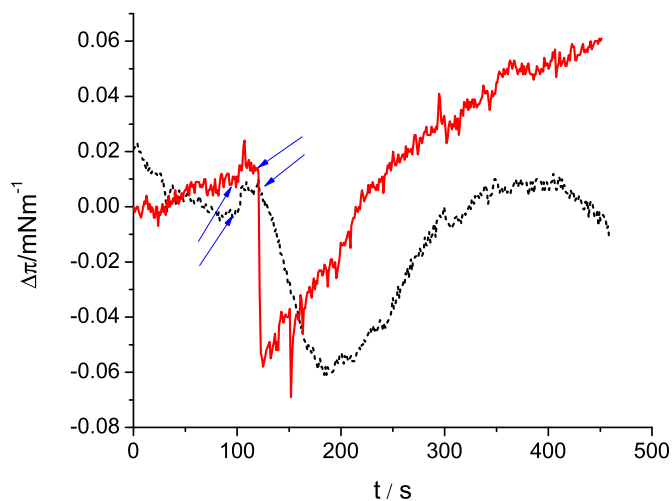


Fig. 3. Variation of surface pressure difference ($\Delta\pi = \pi - \pi_{\text{initial}}$) before and after applying a potential step at $E = 0.250 \text{ V}$ during 30 s. Aqueous phase composition: (dashed line) 10.00 mM LiCl, (full line) 10.00 mM LiCl + 0.50 mM PFN.

increased, a peaked shape voltammogram is observed for the forward process, even for high surfactant concentrations (not shown). Also in this case an abrupt change in current values is observed at surfactant concentration values equal to or greater than 2.24 mM.

From these voltammograms, the dependence of $I_p(-)$, the negative peak current values, on PFN^- concentration was analyzed. In Fig. 5 the variation of $I_p(-)$ measured at $E_1 = 0.425 \text{ V}$ (first process corresponding to monomeric PFN^- transfer) and at

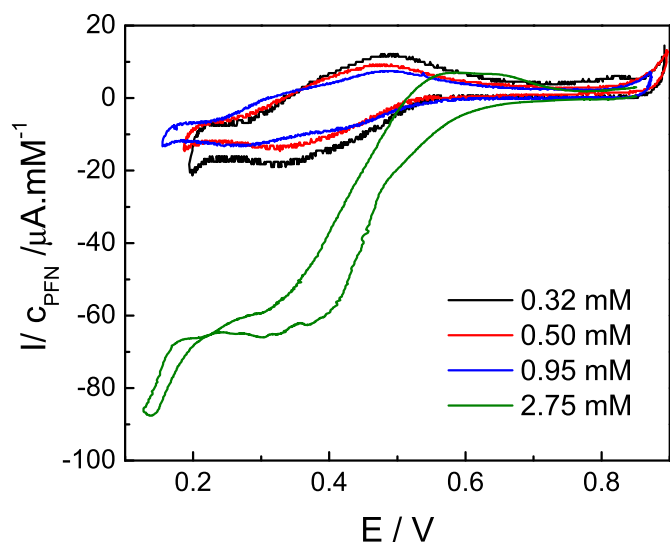


Fig. 4. Cyclic voltammograms for PFN^- transfer at the water/1,2-dichloroethane interface normalized by PFN^- concentration in the aqueous phase. Aqueous phase composition: 10.00 mM LiCl + PFN^- . Organic phase composition: 10.00 mM TPnATCIPhB. $\nu = 0.010 \text{ V s}^{-1}$.

$E_2 = 0.320 \text{ V}$ (second process corresponding to the transfer of pre-micellar species) was plotted vs PFN^- concentration. For this purpose, the first voltammetric peak was fitted to a theoretical reversible and diffusion controlled process, which allowed the determination of the peak current for the second process. As can be noted in Fig. 5, the peak current for PFN^- transfer shows a linear relationship with the anion concentration up to a constant value. In parallel the peak current corresponding to the second process increases linearly with PFN^- concentration up to a value between 2.00 and 2.27 mM, from which a sharp current increase, associated with charged micelles transfer, is observed. This abrupt increase in current values is coincident with the concentration range where constant peak current is observed for the first process, reinforcing the hypothesis that the equilibrium monomeric surfactant/micelle is reached. Thus, from the intercept point between two functions resulting from the linear fit of both data sets measured at E_2 , the critical micellar concentration (cmc) equal to 2.23 mM for PFN^- is

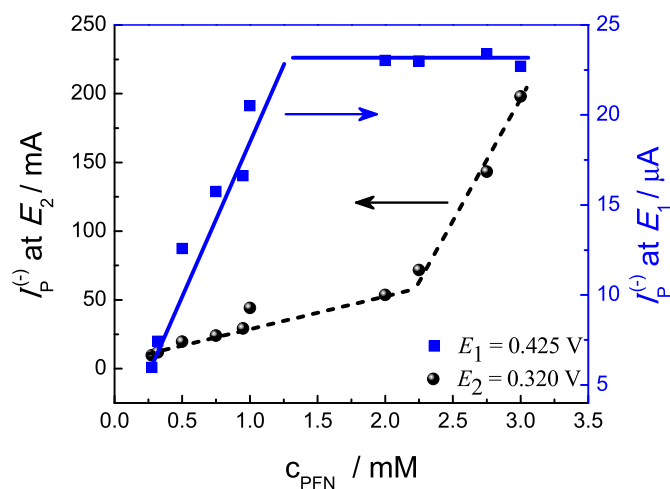


Fig. 5. Variation of I_p at $E = 0.320 \text{ V}$ (●) and $E = 0.425 \text{ V}$ (■) with PFN^- concentration. Aqueous phase composition: 10.00 mM LiCl + PFN^- . Organic phase composition: 10.00 mM TPnATCIPhB. $\nu = 0.050 \text{ V s}^{-1}$.

determined. Similar behavior was obtained for PFO^- and PFD^- and following the same procedure, cmc values were calculated for both surfactants and listed in Table 2. As expected, the highest cmc value was obtained for PFO^- due to its shorter hydrocarbon chain, which leads to lower hydrophobic forces, i.e. lower entropy – dominated association of surfactants in micelles.

3.2. Comparison with cmc values determined by other methods

3.2.1. Surface pressure measurements

Fig. 6a shows the compression isotherm (pressure vs trough area) obtained for PFN^- at 25°C . There is an initial slight decrease of surface pressure, at the beginning of compression, indicating an initial desorption of a small amount of molecules from the surface, which is an already reported behavior for partially water soluble compounds, such as these ionic species [32]. Despite this initial desorption, the increase in pressure observed from area values lower than 100 cm^2 reveals that this ion has an important surface activity. In this way, experiments that allow analyzing the variation of π on surfactant concentration were carried out. For this purpose successive volumes of a solution 1.00 mM PFN^- were added to the subphase containing 10.00 mM LiCl in order to reach PFN^- concentration values within the range $1.00\text{--}3.50 \text{ mM}$. After each injection, the variation of surface pressure on time was recorder (Fig. 6b). The stationary π values measured after each injection were plotted as a function of PFN^- concentration and the results are shown in Fig. 6c. As it can be noted, the increase in surfactant concentration produces an increase in surface pressure, due to PFN^- adsorption, up to a constant value attained when the surface is saturated with surfactants molecules and the micelle formation begins to occur. The concentration value corresponding to the intercept of both linear regressions in Fig. 6c is the cmc. Similar behavior was observed for the other surfactants and cmc values, determined using the present methodology, are listed in Table 2. As can be observed, there is a good correlation between cmc values determined by surface pressure measurements and by cyclic voltammetry.

3.2.2. Fluorescence measurements

Fluorescence experiments were carried out employing 8-anilinoanthracene-1-sulfonate (ANS) as fluorescence probe [33]. It is important to remark that ANS exhibits fluorescence emission only in hydrophobic media, for example, when partitioned into a micelle. Fig. 7 shows the fluorescence intensity of a 0.70 mM ANS solution after the addition of increasing amounts of PFN^- . The abrupt change of the slope observed in the fluorescence intensity vs PFN^- concentration plot is due to the micelle formation and the access of ANS to a more hydrophobic media, where it exhibits fluorescence emission. The concentration value corresponding to the intercept of the linear regressions of both data sets is the cmc. In this way the values reported in Table 2 were determined for PFO^- , PFN^- and PFD^- .

Similarly to the results obtained from surface pressure

Table 2
cmc values for PFO^- , PFN^- and PFD^- determined by surface pressure variation on concentration, fluorescence of ANS and cyclic voltammetry at the water/1,2-dichloroethane interface.

	cmc/Method		
	Surface Pressure	Fluorescence	Cyclic Voltammetry
PFO	$1,11 \cdot 10^{-2} \text{ M}$	$9,91 \cdot 10^{-3} \text{ M}$	$9,4 \cdot 10^{-3} \text{ M}$
PFN	$2,24 \cdot 10^{-3} \text{ M}$	$2,25 \cdot 10^{-3} \text{ M}$	$2,23 \cdot 10^{-3} \text{ M}$
PFD	$2,21 \cdot 10^{-3} \text{ M}$	$2,10 \cdot 10^{-3} \text{ M}$	$2,1 \cdot 10^{-3} \text{ M}$

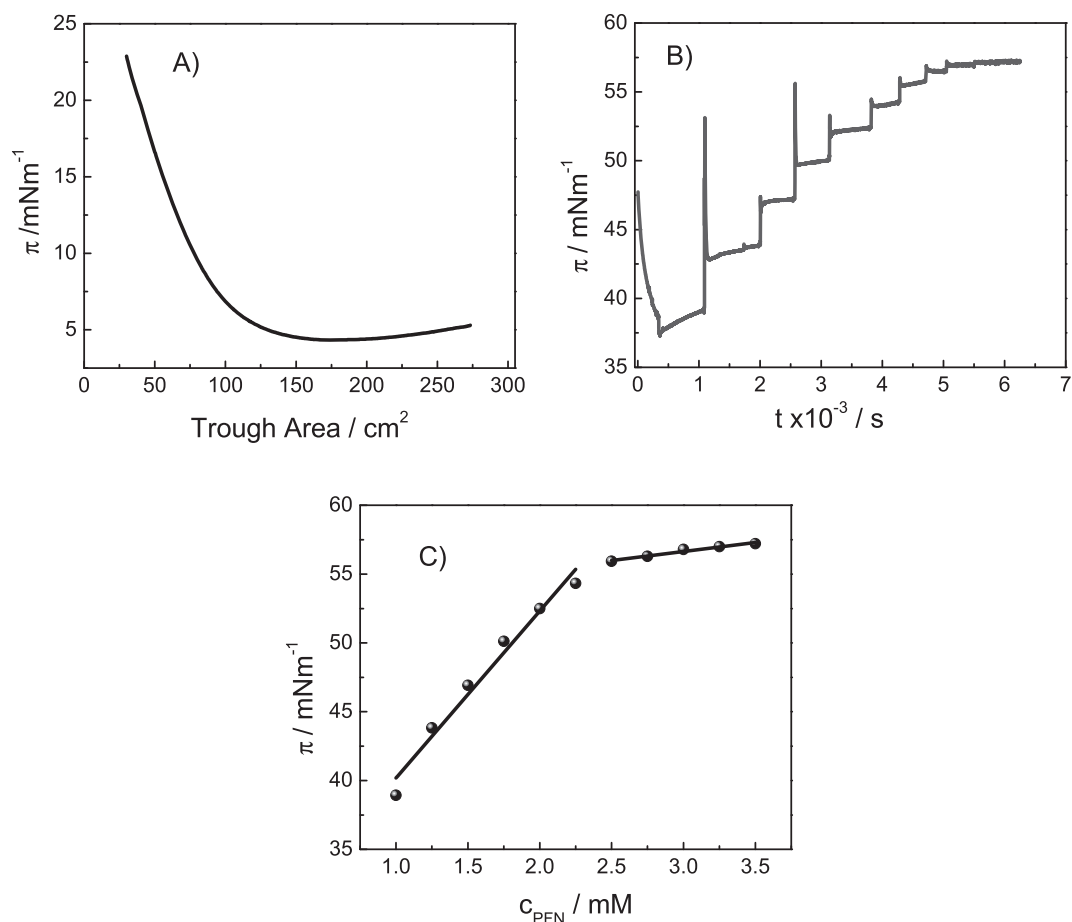


Fig. 6. A) Compression isotherms of PFN^- at air/water interface obtained after the injection of $100\ \mu\text{L}$ of $0.70\ \text{mM}$ PFN solution at the interface. Subphase composition: $10.00\ \text{mM}$ LiCl . B) Variation of surface pressure with time after successive injections of $5\ \mu\text{L}$ $0.10\ \text{M}$ PFN solution into the subphase containing $10.00\ \text{mM}$ LiCl . C) Variation of the stationary surface pressure (π) with PFN concentration in the subphase containing $10.00\ \text{mM}$ LiCl .

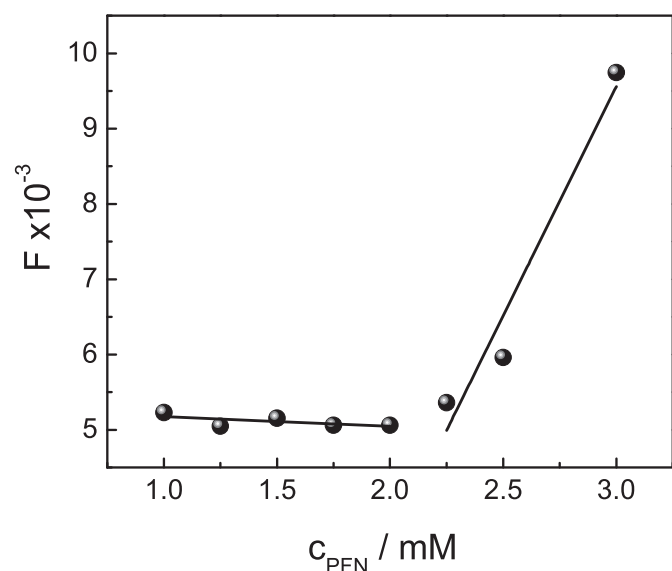


Fig. 7. Variation of fluorescence intensity (F) against PFN concentration. Solution composition: $0.70\ \text{mM}$ Fluorescent probe + PFN at different concentrations from $1.00\ \text{mM}$ to $3.00\ \text{mM}$ + $10.00\ \text{mM}$ LiCl .

measurement, also in this case, the data obtained from fluorescence-based method are in very good agreement with those

derived from cyclic voltammetry. These evidences validate the use of cyclic voltammetry at a liquid/liquid interface as an alternative method for determining cmc values of charged surfactants.

3.3. Electrochemistry impedance spectroscopy (EIS) and capacitance measurements

EIS experiments were carried out to evaluate the interface properties in the presence of high concentrations of the surfactants in aqueous phase. Under these conditions, adsorption of surfactants forming a compact monolayer is expected, and differentiation between homogeneous or heterogeneous film with different domains, should be possible from these experiments. In this way, impedance spectra were recorded in the frequency range $0.1\ \text{Hz} < f < 2\ \text{kHz}$, at two different dc potential values: $E_{\text{dc}} = 0.400\ \text{V}$ (where the surfactant or micelle transfer takes place) and $E_{\text{dc}} = 0.800\ \text{V}$ (where surfactant transfer does not occur), and two PFN^- concentrations in the aqueous phase: $c_1 = 0.25\ \text{mM}$ and $c_2 = 3.00\ \text{mM}$ ($c_1 < \text{cmc} < c_2$). Fig. 8 shows the Nyquist plots obtained under these conditions, together with the fitting results (solid lines) obtained with the equivalent circuits shown in Fig. 8 (c and d). The best circuit fitting the experimental data depends on surfactant concentration. On the one hand for low PFN^- concentrations compared to cmc (c_1) the results were well fitted to the typical Randles circuit (Fig. 8 c), where R_1 is the solution resistance, CPE1 is the constant phase element which takes into account the double layer capacitance (C_{dl}), R_2 is the charge transfer resistance

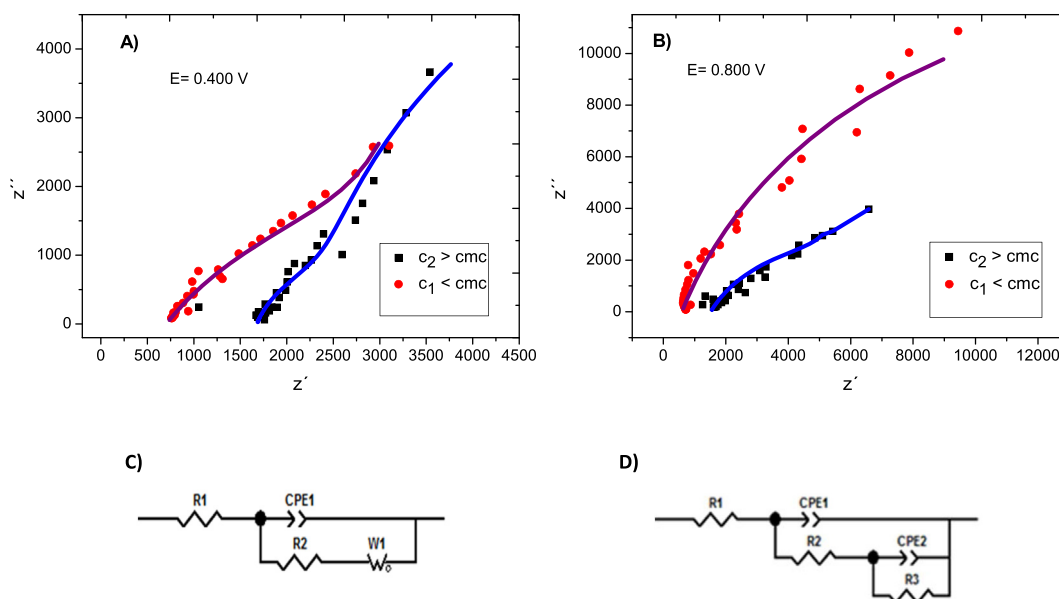


Fig. 8. Nyquist plots, Z'' vs Z' , obtained at (A) $E = 0.400$ V and (B) $E = 0.800$ V. Fitting results are shown in solid line. Aqueous phase composition: 10.00 mM LiCl + (●) 0.25 mM and (■) 3.00 mM PFN. Organic phase composition: 10.00 mM TPnATCIPhB. C) and D): Equivalent circuits employed to fit EIS results.

and the Warburg element, $W1$, was included when $E_{dc} = 0.400$ V was applied to the interface, which models the diffusion process involved in PFN^- transfer. It was not necessary to include this Warburg element for $E_{dc} = 0.800$ V, potential at which the surfactant transfer does not occur. On the other hand, for PFN^- concentrations higher than cmc (c_2), the EIS response could no longer be fitted with a Randles circuit. Instead, the results fit better with the equivalent circuit shown in Fig. 8 d, which can be interpreted by considering the formation of an inhomogeneous film, in which different domains are present, with uncovered zones (bare, without PFN^- molecules) characterized by a charge transfer resistance ($R3$), a double-layer capacitance ($CPE2$) and a solution resistance within the pores ($R2$); and another domains corresponding to covered zones (domains with adsorbed PFN^- molecules) and characterized by a monolayer capacitance ($CPE1$). These findings from the EIS experiments, demonstrating the presence of different domains, are consistent with the steady-state wave response observed for PFN^- transfer at low sweep rates during the negative voltammetric sweep rate, typical for ion transfer at microholes.

Fig. 9 shows the variation of capacitance, C , with potential obtained by a.c. voltammetry at the liquid/liquid interface, for the base solutions in the absence or in the presence of PFN^- in the aqueous phase at concentrations equal to c_1 and c_2 as describes above. As it can be noticed, the curves corresponding to double layer capacitance at the interface between the base electrolytes in the absence or in the presence of low PFN^- concentration (c_1) are almost coincident, except by the maximum observed at $E = 0.450$ V due to the pseudo-capacitance of PFN^- transfer. For PFN^- concentrations higher than cmc (c_2), an important shift of C vs E curves towards more positive potential is observed, which evidences the presence of PFN^- negatively charged molecules adsorbed at the interface at these high surfactant concentrations.

3.4. Determination of the aggregation number

The aggregation number (N) of a micellar aggregate can be determined measuring the change in fluorescence of a probe when it is in the presence (F) or in the absence (F_0) of a quencher (Q) at

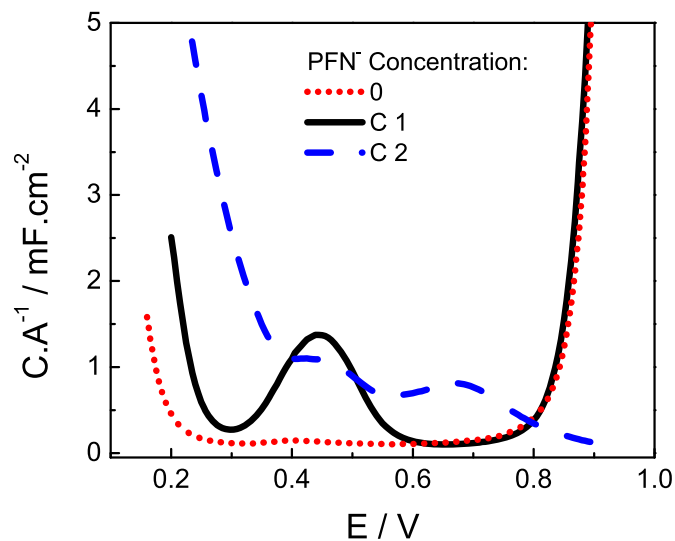


Fig. 9. Plots of Capacitance vs Potential. Aqueous phase composition: (—) 10.00 mM LiCl, (⋯) 10.00 mM LiCl + 0.25 mM PFN and (---) 10.00 mM LiCl + 3.00 mM PFN. Organic phase composition: 10.00 mM TPnATCIPhB.

different quencher concentrations, according to the method reported by N.J. Turro et al. [34]. This method is based on the quenching of a fluorescent probe (P , pyrene in the present work) by a hydrophobic quencher (Q , cetylpyridinium chloride in this work). Both, quencher and probe reside exclusively in the micellar phase, then they are distributed among the available micelles. For a solution containing a surfactant (PFO , PFN or PFD) concentration $[S_0] > cmc$, then monomeric surfactant and micelles, formed by N molecules of surfactant, are both present and the micelle concentration $[M]$ is equal to:

$$[M] = ([S_0] - cmc) / N \quad (1)$$

If the quencher is present in the same solution, at a

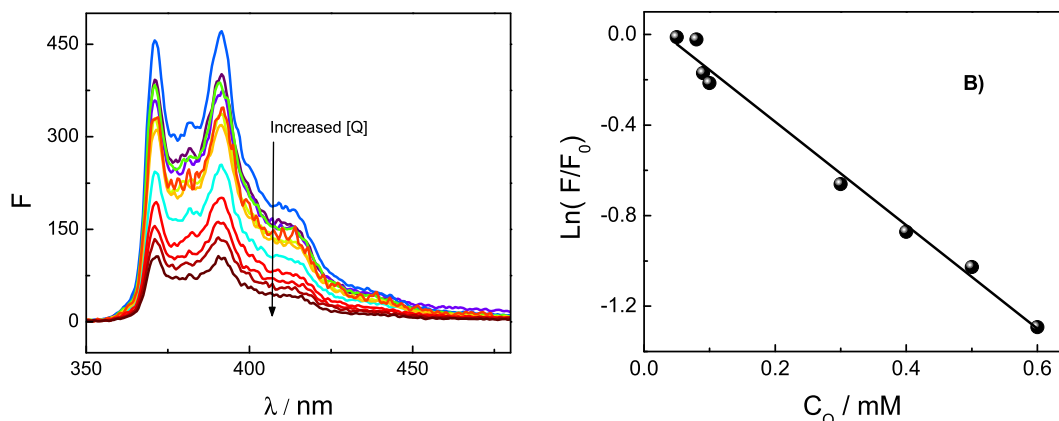


Fig. 10. **A)** Pyrene spectrum at different concentration of quencher (cetylpyridinium bromide). Solution composition: 2.0 μM Pyrene + Quencher at different concentrations from 50.0 μM to 600.0 μM + 4.00 mM PFN + 10.00 mM LiCl. **B)** Plot of $\ln(F/F_0)$ for Pyrene as a function of quencher concentration.

concentration $[Q]$, and the probe is added to the system, it will partition among micelles containing Q and among “empty” micelles. Poisson statistics can describe the distribution of probe and quencher among micelles in this tertiary system. If the probe is fluorescent only when it occupies an empty micelle (and fluorescence is completely quenched when it occupies a micelle containing at least one Q molecule), then the measured ratio of fluorescence intensities (F/F_0) in the presence of Q respect to that in the absence of Q is related by:

$$F/F_0 = \exp(-[Q]/[M]) \quad (2)$$

Then, a decrease of F with quencher concentration is expected. By combination of Equations (1) and (2), the following expression is obtained:

$$\ln \frac{F}{F_0} = - \frac{[Q] \cdot N}{[S_0] - CMC} \quad (3)$$

In this way, the logarithm of the ratio between the integrated area from each fluorescence spectrum of pyrene in the presence or in the absence of the quencher for each surfactant (Fig. 10a for PFN⁻), was plotted against the quencher concentration (Fig. 10b for PFN⁻) and from the slope of the plot, the value of N was calculated. Similar plots were obtained for PFO⁻ and PFD⁻. The resulting N values were 12, 9 and 5 molecules/micelle for PFO⁻, PFN⁻ and PFD⁻ respectively. Although these values may seem very small, a similar aggregation number was previously determined by Turro and Lee for micelles of sodium perfluorooctanoate ($N = 7$ molecules/micelle) [35], and in that work, the authors mentioned the formation of “mini” micelles of this surfactant in contrast to the typical micelles of hydrocarbon surfactants that normally presents higher N values. There is a good linear correlation between N and the number of carbons in the perfluorinated chain ($r^2 = 0.9932$, not shown).

Once N values have been calculated, it was possible to determine diffusion coefficient values for micelles of the three surfactants analyzed from the variation of current peak with surfactant concentration (Fig. 5) within the concentration range 2.10 mM < c < 3.00 mM. The results are listed in Table 1 and they are in the same magnitude order than those reported by T. Asakawa et al. [7] for PFN micelles.

4. Conclusions

Taking into account the results obtained in the present paper,

we propose cyclic voltammetry at liquid/liquid interfaces as an useful methodology for the determination of cmc of charged surfactants provided they can be transferred across the interface. The cmc values are evaluated from the abrupt change in voltammetric current, in addition to a change in the shape of the voltammogram as the surfactant concentration is increased. The obtained values were in good agreement with those determined in the present paper by conventional methods. In the same way, the diffusion coefficient of the micelles could be determined from current values, provided previous evaluation of the aggregation number by spectrofluorimetric methods. Impedance spectroscopy experiments showed that at high surfactants concentrations a heterogeneous monolayer of the surfactant, with bare and covered domains, is formed at the liquid/liquid interface.

Besides the possibility of determining important parameters of micelles by this methodology, the results obtained in this paper contribute to the knowledge of the behavior of surfactants and micelles at an interface formed by two immiscible solvents, which is particularly important considering that the main applications of micellar species are based on the transport of different substances through different mediums, changing from polar to non-polar environment, which can modified their nature. The possibility of handling the entry and exit of these species from water to the organic solvent, and vice versa, applying a potential difference, is an interesting strategy to predict the behavior of micelles in such interfaces.

Acknowledgements

Financial support from the Consejo Nacional de Investigaciones Científicas y Tecnológicas (CONICET, PIP 112-201101-00011), the Secretaría de Ciencia y Tecnología de la Universidad Nacional de Córdoba (SECyT - UNC) and the Agencia Nacional de Promoción Científica y Tecnológica (ANPCyT, FONCyT PICT- Raices grant 2013-0822) is gratefully acknowledged. B.N. Viada and E.M. Pachón Gómez thank ANPCyT and CONICET for the fellowships granted.

References

- [1] A. Patist, S.G. Oh, R. Leung, D.O. Shah, *Colloid Surf. A* 176 (2001) 3–16.
- [2] W.C. Preston, *J. Phys. Colloid Chem.* 52 (1948) 84–96.
- [3] P. Mukerjee, K.J. Mysels, *Critical Micelle Concentrations of Aqueous Surfactant Systems*, NSRDS-NBS 36, US Department of Commerce, Washington, DC, 1971.
- [4] M.J. Rosen, *Surfactants and Interfacial Phenomena*, second ed., Wiley, New York, 1989.
- [5] N.M. van Os, J.R. Haak, L.A. Rupert, *Physico-chemical Properties of Selected Anionic, Cationic and Nonionic Surfactants*, Elsevier, Amsterdam, 1993.

- [6] P.G. Molina, J.J. Silber, N.M. Correa, L. Sereno, J. Phys. Chem. C 111 (2007) 4269–4276.
- [7] T. Asakawa, H. Sunagawa, S. Miyagishi, Langmuir 14 (1998) 7091–7094.
- [8] A.B. Mandal, B.U. Nair, D. Ramaswamy, Langmuir 4 (1998) 736–739.
- [9] J.S. Florez Tabares, N.M. Correa, J.J. Silber, L.E. Sereno, P.G. Molina, Soft Matter 11 (2015) 2952–2962.
- [10] C.I. Camara, M.V. Colqui Quiroga, N. Wilke, A. Jimenez-Kairuz, L.M. Yudi, Electrochim. Acta 94 (2013) 124–133.
- [11] H. Janchenova, A. Lhotský, K. Stulik, V.J. Marecek, J. Electroanal. Chem. 601 (2007) 101–106.
- [12] L.M.A. Monzon, L.M. Yudi, Electrochim. Acta 52 (2007) 6873–6879.
- [13] M.V. Colqui Quiroga, L.M.A. Monzon, L.M. Yudi, Electrochim. Acta 56 (2011) 7022–7028.
- [14] M.A. Mendez, Z. Nazemi, I. Uyanik, Y. Lu, H.H. Girault, Langmuir 27 (2011) 13918–13924.
- [15] V. Marecek, A. Lhotsky, H. Janchenova, J. Phys. Chem. B 107 (2003) 4573–4578.
- [16] A.K. Kontturi, K. Kontturi, L. Murtomaki, B. Quinn, V.J. Cunnane, J. Electroanal. Chem. 424 (1997) 69–74.
- [17] M. Nakagawa, N. Sezaki, T. Kakiuchi, J. Electroanal. Chem. 501 (2001) 260–263.
- [18] V. Marecek, H. Jänchenová, J. Electroanal. Chem. 558 (2003) 119–123.
- [19] H. Jänchenová, K. Stulik, V. Marecek, J. Electroanal. Chem. 591 (2006) 41–45.
- [20] L. Poltorak, K. Morakchi, G. Herzog, A. Walcarius, Electrochim. Acta 179 (2015) 9–15.
- [21] L. Poltorak, G. Herzog, A. Walcarius, Langmuir 30 (2014) 11453–11463.
- [22] L. Poltorak, M. Dossot, G. Herzog, A. Walcarius, Phys. Chem. Chem. Phys. 16 (2014) 26955–26962.
- [23] M.Y. Vagin, E.V. Malyh, N.I. Larionova, A.A. Karyakin, Electrochem. Commun. 5 (2003) 329–333.
- [24] P. Mukerjee, T. Handa, J. Phys. Chem. 85 (1981) 2298–2303.
- [25] H. Kunieda, K. Shinoda, J. Phys. Chem. 80 (1976) 2468–2470.
- [26] J.L. Lopez-Fontan, F. Sarmiento, P.C. Schulz, Colloid Polym. Sci. 283 (2005) 862–871.
- [27] M.F. Torres, R.H. de Rossi, M.A. Fernandez, J Surfact Deterg 16 (2013) 903–912.
- [28] J. Lipkowski, in: B.E. Conway, et al (Eds.), Modern Aspects of Electrochemistry vol. 23, Plenum Press, New York, 1992, p. 8.
- [29] H. Reller, E. Sabatini, I. Rubinstein, J. Phys. Chem. 91 (1987) 6663.
- [30] H. Reller, E. Kirova-Eisner, E. Gileadi, J. Electroanal. Chem. 138 (1982) 65.
- [31] C. Amatore, J.M. Saveant, D. Tessier, J. Electroanal. Chem. 147 (1983) 39.
- [32] G.L. Gaines, Insoluble Monolayers at Liquid–Gas Interfaces” Chapter 4, Section III (Pages 151–154), John Wiley and Sons, Inc., New York (, 1966.
- [33] E.B. Abuin, E.A. Lissi, A. Aspee, F.D. Gonzalez, J.M. Varas, J. Colloid Interface Sci. 186 (1997) 332–338.
- [34] N.J. Turro, A. Yekta, J. Am. Chem. Soc. 100 (1978) 5951–5952.
- [35] N.J. Turro, P.C.C. Lee, J. Phys. Chem. 86 (1982) 3367–3371.